Förster transfer and the local optical density of states in erbium-doped silica

M. J. A. de Dood,[1,2,*] J. Knoester,[3] A. Tip,[1] and A. Polman[1]

[1]*FOM Institute for Atomic and Molecular Physics, Kruislaan 407, 1098 SJ Amsterdam, The Netherlands*
[2]*Department of Physics, University of California—Santa Barbara, Santa Barbara, California 93106, USA*
[3]*Institute for Theoretical Physics and Materials Science Center, University of Groningen, Nijenborgh 4,*
9747 AG Groningen, The Netherlands
(Received 6 December 2004; published 4 March 2005)

Optically excited erbium ions incorporated near the surface of a silica glass decay by spontaneous emission and—at high Er concentration—via Förster energy transfer to quenching sites. By externally modifying the photonic microstructure we vary the local optical density of states (LDOS) in samples with different degrees of Förster transfer. Changes in spontaneous emission rate are consistent with calculated variations in LDOS at 1.5 μm, while Förster energy transfer is not affected by the LDOS. The latter is attributed to the fact that Förster transfer involves virtual photons with a broad energy spectrum, excluding a special role for the LDOS at the atom's transition frequency.

I. INTRODUCTION

Resonant excitation energy transfer between atoms or molecules is a well-known and important phenomenon in physics, chemistry, and biology. The nature of the transfer depends on the distance r between the atoms. If r is large compared to the emission wavelength, energy transfer takes place via emission and reabsorption of real photons, described by the far-field radiative interaction and a rate that scales as $1/r^2$. For distances small compared to the emission wavelength, the near-field contribution dominates. For dipole-allowed transitions this leads to the well-known $1/r^6$ rate of Förster energy transfer,[1] the dominant excitation energy transport process at the nanometer scale. Förster transfer plays a key role in biological processes such as photosynthesis,[2] and is important in nanometer-scale photonic and electromagnetic applications, such as highly doped light-emitting diodes and lasers, or plasmon wires.[3] Alternatively, it is important in schemes for quantum computation that involve storage and transfer of quantum information in the solid state.[4]

Clearly, control of Förster energy transfer would open many interesting possibilities to control the excitation dynamics and optical functionality at the nanometer scale. One way of achieving this is to control the relative positions of the atoms or molecules that carry the excitations.[5] In a microstructured dielectric environment the spontaneous emission rate is modified by variation in the local optical density of states (LDOS) thereby changing the competition between Förster transfer and spontaneous decay. When spontaneous emission is completely inhibited, as can be the case in a photonic crystal,[6] Förster transfer may dominate the excited-state dynamics completely. The effect of LDOS on spontaneous emission was first noticed by Purcell[7] and today many examples exist where the rate of emission is altered by a dielectric structure.[8–11] Indeed, the LDOS at the atomic transition energy E_0 is the key quantity in all these examples[12,13] as follows directly from Fermi's golden rule.

An intriguing and highly debated question is whether the LDOS also affects the Förster rate itself as was, e.g., suggested in Ref. 14. At the quantum-electrodynamic level, electromagnetic interactions are described by the exchange of photons between two atoms.[15,16] However, these photons do not obey energy conservation. As they merely constitute intermediate (virtual) states in the process, which exist for a finite time Δt, the uncertainty principle $\Delta E \Delta t \geq \hbar$ allows for a spread in their energies. Taking for the typical time Δt the travel time r/c of photons between the two atoms (c is the velocity of light), one arrives at an estimate for the energy spread of $\Delta E \geq \hbar c/r$. In the far-field region, $r \gg \hbar c/E_0$, and thus $\Delta E \ll E_0$, the LDOS at the energy E_0 dominates the energy transfer and may be regarded as emission and reabsorption of a real photon.

However, at the nanometer scale, relevant to Förster transfer, the photons taking part in the energy transfer are spread over an energy interval $\Delta E \geq E_0$. This implies that the LDOS at the energy E_0 does not play a special role. Rather, one expects that modifying the LDOS will only affect the rate of Förster transfer if the LDOS averaged over an energy region that is large compared to a typical optical energy differs from its vacuum value. For example, one does not expect that control of the Förster transfer rate is possible in photonic crystals,[16] because the LDOS averaged over a large frequency range closely follows the smooth energy-squared dependence typical for a homogeneous dielectric.

II. EXPERIMENT

Here, we present experimental proof of the fact that in general modification of the LDOS does not affect Förster transfer by studying a set of soda lime silicate glass samples doped with erbium ions similar to those used in previous studies.[9,17] These samples provide an excellent model system in which the Förster transfer rate and the LDOS can be varied independently. Trivalent erbium ions show optical transitions around 1.536 μm between the $^4I_{13/2}$ and $^4I_{15/2}$ intra-4f states. As this transition is parity forbidden, the radiative lifetime of Er in silica is relatively long, 10–20 ms. In concentrated systems ($>$0.1 at. % Er) concentration quenching
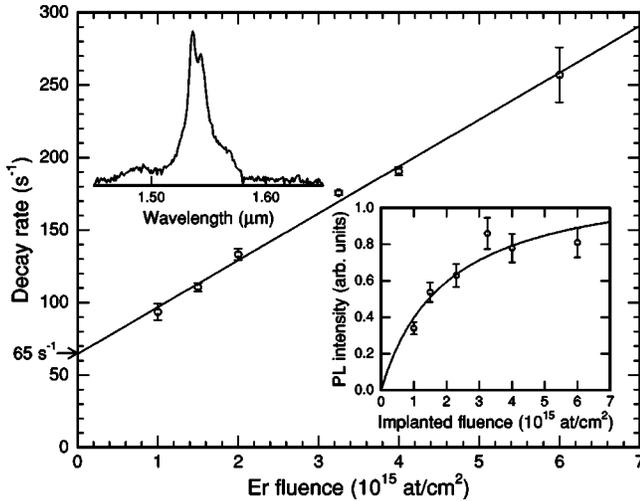
FIG. 1. Photoluminescence decay rate at 1.536 μm of Er^{3+} ions in soda lime silicate glass as a function of the implanted Er fluence. The solid line through the data describes a linear concentration quenching model and extrapolates to a value of 65 ± 4 s^{-1} close to the radiative rate of Er^{3+} in soda lime silicate glass (62 ± 4 s^{-1}). The insets show the PL spectrum (upper left corner) and the PL intensity at 1.536 μm as a function of implantation fluence (lower right corner), measured in the linear pump regime.

becomes apparent: energy can migrate through the glass by Förster transfer between the closely spaced Er^{3+} ions until a quenching center is met. In our experiment the Förster transfer rate is modified by varying the Er concentration, while the LDOS is varied by immersing samples in liquids with different refractive indices, a method we have developed earlier to study low concentration samples.[9,10] Here, we extend the method to higher concentration samples to obtain a consistent set of data that allows us to study the effect of the LDOS on the Förster transfer process.

The samples in this study were prepared by implantation of 500 keV Er ions into the near-surface region of soda lime silicate glass samples. Samples with different areal densities in the range $(1-6)\times10^{15}$ at/cm^2 were prepared and annealed for 1 h at 512 °C in vacuum. The erbium depth distribution as measured by Rutherford backscattering spectrometry is Gaussian shaped, with a peak at a depth of 103 nm and a width $\sigma=43$ nm. Infrared photoluminescence (PL) spectra were recorded at room temperature using the 488 nm line of an Ar ion laser as the excitation source. Standard lock-in techniques were used by modulating the laser beam with an acousto-optic modulator at a frequency of 7 Hz. A representative PL spectrum is shown in an inset of Fig. 1. It shows the emission from the Stark-split $^4I_{13/2}\rightarrow{}^4I_{15/2}$ intra-$4f$ transitions of Er^{3+}. PL decay traces were recorded using a digitizing oscilloscope. The time resolution of the system was ~30 μs, limited by the Ge detector response.

III. VARYING THE NONRADIATIVE DECAY RATE

Figure 1 shows the $1/e$ PL decay rate measured at 1.536 μm for samples implanted with different Er fluences. The decay rate increases linearly from 100 s^{-1} for the lowest

fluence to 250 s^{-1} for the highest fluence. This linear increase with concentration is observed in many cases and can only be modeled assuming Förster energy transfer between the Er^{3+} ions on a microscopic scale. Resonant transfer among Er^{3+} ions does not alter the decay rate of the excited ensemble unless there is a small concentration of quenchers in the glass. Once the energy is transferred to such a quencher the energy is lost from the Er^{3+} system and the decay is nonradiative. When the density of Er^{3+}(N_{Er}) is much larger than the density of quenchers (N_q), diffusion of the excitation between the Er^{3+} ions is the rate limiting step. In this limit, the solution of the three-dimensional diffusion equation leads to near single-exponential decay with a total decay rate given by[18,19]

$$W = W_{rad} + W_{nr,int} + 4\pi C_{Er,Er}N_qN_{Er}, \tag{1}$$

where W_{rad} is the radiative decay rate of the erbium ions, $W_{nr,int}$ is the intrinsic nonradiative rate, and $C_{Er,Er}$ is an Er-Er interaction constant. The linear dependence on N_{Er} in Eq. (1) follows directly from the $1/r^6$ dependence of the microscopic Förster energy transfer process.[19] For Er^{3+} in glass the luminescence is quenched by –OH impurities and their density can be found independently from infrared absorption spectra to be $\sim10^{19}$ /cm^3,[17] indeed 10–100 times lower than the Er concentration range studied here.

The inset of Fig. 1 shows the measured PL intensity at 1.536 μm as a function of implanted Er fluence. The data were taken in the low pump power regime, where the PL intensity is proportional to the product of Er fluence and emission quantum efficiency W_{rad}/W. The solid line uses the measured linear increase of the total decay rate, assuming that the radiative rate is constant and provides an excellent description of the observed saturation of PL intensity. Thus, the increased decay rate for increasing Er fluence is due to an increase in the nonradiative component due to Er-Er interaction (and not due to an increased radiative rate). Precipitation of Er can be excluded as we have shown before,[17] because metallic precipitates do not luminesce, and would lead to a decrease in PL intensity without changing the decay rate.

IV. MODIFYING THE RADIATIVE DECAY RATE

Having prepared samples with different nonradiative rates and having identified their decay mechanism we can now address the modification of the radiative rates. Because the Er^{3+} atoms are localized close to the surface their optical environment can be varied by changing the refractive index outside the glass. The resulting change in reflective properties of the interface will then change the LDOS at the position of the Er^{3+} ions. The relation between the LDOS and the radiative rate is obtained from Fermi's golden rule using the electrical dipole approximation to describe the coupling between the atom and the electromagnetic field:[12,13]

$$W_{rad} = \frac{2\pi}{\hbar}D^2 f(\omega,z), \tag{2}$$

where D is a matrix element of the atomic transition involved and $f(\omega,z)$ is the LDOS, normalized to the LDOS in
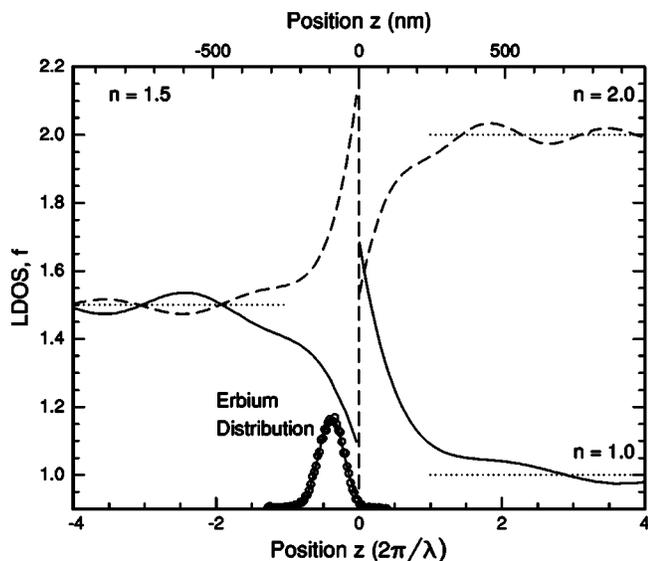
FIG. 2. Calculated LDOS for soda lime silicate glass, normalized to the LDOS of a bulk medium with refractive index 1.0, as a function of distance from the interface at $z=0$. The LDOS is shown for glass ($n=1.5$) in contact with air ($n=1.0$, solid line) or in contact with a medium with $n=2.0$ (dashed line). The measured Er depth distribution is indicated as well. The LDOS at the position of the Er ions is modified by the index of the outside medium. The top axis shows a distance scale corresponding to the emission wavelength of Er (1.536 μm).

vacuum, for a transition frequency ω at a distance z from the interface. In our case the transition frequency is fixed by the transition of the Er^{3+} ion and it suffices to consider the LDOS at a single frequency only. The LDOS is calculated using a complete set of normalized eigenfunctions for the macroscopic Maxwell equations. These are constructed using the Fresnel coefficients for reflection and refraction of plane waves at an interface.[9,12] Local-field effects are included in the matrix element D since the microscopic field at the position of the Er^{3+} atoms is only varied through the macroscopic E field.

Figure 2 shows the calculated LDOS as a function of distance from the interface for soda lime silicate glass ($n=1.5$) in contact with air ($n=1.0$) and a medium with $n=2.0$. The bottom axis indicates the distance in units $\lambda/2\pi$, where λ is the emission wavelength. The corresponding depth scale for Er^{3+} emission at 1.536 μm is indicated on the top axis. The measured Er depth profile is indicated by the open circles. As can be seen the LDOS close to the interface, at the position of the Er^{3+} ions, is strongly dependent on the optical properties of the interface. Faraway from the interface the normalized LDOS approaches the bulk value, which is equal to the refractive index of the medium. The oscillations observed close to the interface have a periodicity of $\sim\lambda/2n$ and are related to interference from incoming and reflected waves.

Figure 3 shows PL decay rates measured for a single sample (1×10^{15} Er/cm^2) brought into contact with air ($n=1.0$) and with various transparent liquids with refractive indices ranging from 1.33 to 1.63. Time-resolved decay measurements for the sample in contact with air and in contact
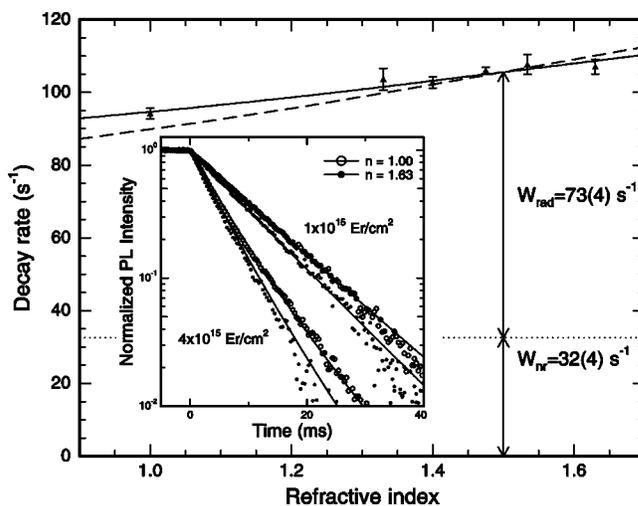

FIG. 3. Measured PL decay rate at 1.536 μm for a sample implanted with 1×10^{15} Er/cm^2 in contact with a range of liquids with different refractive indices. The decay rate increases with increasing refractive index. The depth-integrated effect of the LDOS (see Fig. 2) assuming that all decay is radiative is shown by the dashed line. The solid line is a fit allowing for nonradiative decay at a rate $W_{nr}=32\pm4$ s^{-1} (dotted line) and leads to a radiative rate at $n=1.5$ of 73 ± 4 s^{-1}. The inset shows measured decay curves for samples in contact with air and with a liquid with a refractive index of 1.63 implanted with 1×10^{15} Er/cm^2 and 4×10^{15} Er/cm^2. The solid lines are fits to the experimental data using the model described in the text.

with a liquid with $n=1.63$ are shown in the inset. The data can be fit by single-exponential decay curves with decay rates of 93 ± 2 s^{-1} and 106 ± 2 s^{-1}, respectively.

V. DISCUSSION

As can be seen in Fig. 3 the measured decay rate increases with the refractive index of the liquid, in qualitative agreement with the increased LDOS at the location of the Er^{3+} ions calculated in Fig. 2. To obtain a quantitative comparison between data and theory, the LDOS was integrated over depth, weighing the contribution from different depths using the measured Er depth profile. This curve was normalized (as the LDOS only does not provide an absolute scale) to the measured decay rate at $n=1.5$. The result is indicated by the dashed line in Fig. 3. The experimental data show a much weaker dependence on refractive index, an effect that we have systematically observed for a large range of Er-implanted glasses.[9,10] This implies that a nonradiative decay component must be invoked that is not influenced by the LDOS. The best fit to the data including this nonradiative decay is shown by the solid line in Fig. 3 and yields a nonradiative rate of 32 ± 4 s^{-1} and a radiative rate of 73 ± 4 s^{-1} at $n=1.5$ (bulk glass).

For the sample in air ($n=1.0$) the fit in Fig. 3 gives a radiative rate of 62 ± 4 s^{-1}. This value is in perfect agreement with the extrapolation of the data in Fig. 1 to zero Er concentration, i.e., where no Förster transfer occurs and thus the decay is purely radiative. As there is no nonradiative decay

component at zero Er concentration, the nonradiative contribution derived from Fig. 3 is caused by Förster transfer. This implies that Forster transfer is not linear in the LDOS at the transition frequency. Taking into account the error bars, the 20% variation in LDOS imposed in our experiment leads to an effect on the energy transfer rate of $0 \pm 4\%$, well outside the 20% value.

To further support this claim we investigate decay traces at high Er^{3+} concentration where Förster transfer causes the dominant decay process to be nonradiative. The inset of Fig. 3 shows decay traces for the sample implanted with 4×10^{15} Er/cm^2 measured in air (open symbols) and in contact with a liquid with $n = 1.63$ (closed symbols). Again a significant effect of the liquid's index on the decay rate is observed. The decay curves are clearly non-single-exponential as at this high Er^{3+} concentration the decay rate varies strongly with depth due to the varying Er^{3+} concentration with depth. To describe the measured decay curves as a superposition of decay traces from Er^{3+} at different depths, the effects of LDOS and concentration quenching (leading to an enhanced decay rate, and a reduced quantum efficiency) were integrated over depth, taking into account the known Er^{3+} concentration profile and the nonradiative rate as a function of Er^{3+} concentration from Fig. 1. This approximate model that assumes a diffusion length much smaller than the width of the Er distribution is valid as the distance between the –OH quenchers (5 nm for $N_q = 10^{19}$ at/cm^3) is much smaller than the width of the Er distribution. The result of this superposition is shown by the solid lines. Note that this model introduces no new parameters and provides a good description of the data in the inset of Fig. 3.

The fact that a sizable effect of refractive index on the decay is observed in these high-concentration samples even though their decay is dominated by nonradiative processes deserves special attention. The PL intensity collected from each depth of the sample is proportional to the number of Er^{3+} ions times the quantum efficiency W_{rad}/W. In the high concentration sample, the LDOS does not have a profound influence on the total decay rate at the peak of the Er distribution, since $W_{rad} \ll W$. However the effect on the emitted PL intensity is large (proportional to W_{rad}/W).[20] In the tails of the Er distribution where $W_{rad} \sim W$, the change in the total decay rate is large, but the change in emitted PL intensity is small, because a lower decay rate leads to a higher steady state Er^{3+} population.[11,20] The shorter decay time in the concentrated sample when immersed in a liquid is thus mostly due to the increased relative PL contribution from Er^{3+} ions at the peak of the distribution.

VI. CONCLUSIONS

Our experimental findings contradict an earlier claim that there is a linear relation between Förster transfer and the LDOS at the transition frequency for dye molecules in a microcavity.[14] Following the discussion in the Introduction, the typical frequency range that is relevant for the virtual transitions describing Förster transfer is c/r. For a typical distance of 3 nm between Er^{3+} ions in our sample this corresponds to a frequency range 100 times larger than the transition frequency. A similar estimate using a distance of 15 nm and emission frequency of 611 nm as given in Ref. 14 leads to a frequency range that is still considerably (six to seven times) larger than the transition frequency, so that our theoretical argument predicts no special role of the LDOS at the transition frequency, despite what is claimed in Ref. 14. One possible alternative explanation for the experimental enhancement found in Ref. 14 may be that the metal mirror causes variations in LDOS over a large spectral range. The use of metals in a micron-sized cavity can influence the electromagnetic mode density over a large frequency range and, e.g., leads to the attractive Casimir force.[21] One possible explanation of the effects measured in Ref. 14 is that they are due to such a broad spectral variation of the mode density between the mirrors. As argued above, those results cannot be explained by variations in just the mode density over the frequency range of the optical transition. A complete calculation of the mode density between mirrors lies outside the scope of our current work.

The detailed analysis of concentration quenching in a model system of Er^{3+} ions in soda lime silicate glass presented in this paper demonstrates that Förster energy transfer does not depend on the LDOS at the transition frequency of the Er^{3+} ions. The fact that the relative contribution of radiative and nonradiative (Förster) processes can be influenced by changing the LDOS can lead to interesting novel concepts of nanoscale energy transfer. For example, if an erbium-doped material is embedded in a photonic crystal with small LDOS, Förster transfer becomes the main decay process. As it involves migration (but not necessarily annihilation) of the excitation, Förster transfer can then lead to the diffusion of an excitation over exceptionally large distances.

*Corresponding author. Electronic address: mdedood@molphys.leidenuniv.nl
[1] T. Förster, Discuss. Faraday Soc. **27**, 7 (1959).
[2] M. Calvin, Rev. Mod. Phys. **31**, 147 (1959).
[3] S. A. Maier, P. G. Kik, H. A. Atwater, S. Meltzer, E. Harel, B. E. Koel, and A. A. G. Requicha, Nat. Mater. **2**, 229 (2003).
[4] A. Imamoglu, D. D. Awschalom, G. Burkard, D. P. DiVincenzo, D. Loss, M. Sherwin, and A. Small, Phys. Rev. Lett. **83**, 4204 (1999).
[5] A. Bar-Haim, J. Klafter, and R. Kopelman, J. Am. Chem. Soc. **119**, 6197 (1997).
[6] E. Yablonovitch, Phys. Rev. Lett. **58**, 2059 (1987).
[7] E. M. Purcell, Phys. Rev. **69**, 681 (1946).
[8] K. H. Drexhage, J. Lumin. **1-2**, 693 (1970).
[9] E. Snoeks, A. Lagendijk, and A. Polman, Phys. Rev. Lett. **74**, 2459 (1995).

[10] M. J. A. de Dood, L. H. Slooff, A. Polman, A. Moroz, and A. van Blaaderen, Phys. Rev. A **64**, 033807 (2001).

[11] A. F. Koenderink, L. Bechger, H. P. Schriemer, A. Lagendijk, and W. L. Vos, Phys. Rev. Lett. **88**, 143903 (2002).

[12] K. Khosravi and R. Loudon, Proc. R. Soc. London, Ser. A **433**, 337 (1991).

[13] B. A. van Tiggelen and E. Kogan, Phys. Rev. A **49**, 708 (1994).

[14] P. Andrew and W. L. Barnes, Science **290**, 785 (2000).

[15] J. Knoester and S. Mukamel, Phys. Rev. A **40**, 7065 (1989).

[16] G. Juzeliunas and D. Andrews, Adv. Chem. Phys. **112**, 357 (2000).

[17] E. Snoeks, G. N. van den Hoven, and A. Polman, J. Appl. Phys. **73**, 8179 (1993).

[18] P. G. de Gennes, J. Phys. Chem. Solids **7**, 345 (1958).

[19] M. J. Weber, Phys. Rev. B **4**, 2932 (1971).

[20] M. J. A. de Dood, A. Polman, and J. G. Fleming, Phys. Rev. B **67**, 115106 (2003).

[21] S. K. Lamoreaux, Phys. Rev. Lett. **78**, 5 (1997).